# Surface-Enhanced Raman Spectroscopy Sensors from Nano-Biosilica with Self-Assembled Plasmonic Nanoparticles

Fanghui Ren, *Student Member, IEEE,* Jeremy Campbell, Gregory L. Rorrer, and Alan X. Wang

***Abstract*—we present an innovative surface-enhanced Raman spectroscopy (SERS) sensor based on a biological-plasmonic hybrid nanostructure by self-assembling silver (Ag) nanoparticles into diatom frustules. The photonic-crystal-like diatom frustules provide a spatially confined electric field with enhanced intensity that can form hybrid photonic-plasmonic modes through the optical coupling with Ag nanoparticles. The experimental results demonstrate 4-6× and 9-12× improvement of sensitivities to detect the Raman dye for resonance and nonresonance SERS sensing, respectively. Such low-cost and high-sensitivity SERS sensors have significant potentials for label-free biosensing.**

***Index Terms*— Diatom frustules, Surface plasmons, Photonic crystals, Surface enhanced Raman spectroscopy**

## I. Introduction

Surface-enhanced Raman spectroscopy (SERS) has been widely investigated as an analytical tool for the detection of various biological and chemical molecules with single molecular sensitivity due to the strong electric fields induced by plasmonic resonances [1]-[2]. Even though an enhancement factor (EF) as large as $10^{14}$ has been report by comparing the measured SERS cross-section of a molecule in the hot-spot to a typical Raman scattering cross-section, controlling the location and density of such hot-spots remains a major challenge for reliable SERS sensing [3,4]. Moreover, increasing the average EF of the whole SERS substrate is even more desirable than obtaining a few extremely strong but very rare hot spots, as the former device can increase the detection probability while reducing the excitation laser power and the integration time for high-throughput optical sensing applications. It has been theoretically proved and experimentally confirmed that placing metallic nanoparticles (NPs) near or inside dielectric microcavities can form hybrid photonic-plasmonic modes [5]-[6], which will further increase the Quality-factors and the local electric field. This concept has been successfully applied to SERS sensing by decorating dielectric ring resonators and photonic crystals with metallic NPs [7]-[9]. In these hybrid nanostructures, the guided-mode resonances (GMRs) of the photonic crystal slab efficiently couple to the localized surface plasmons (LSPs) of the metallic nanostructures, resulting in a higher local electric field to enhance the SERS signals. However, such artificial photonic crystals require top-down fabrication techniques such as optical lithography and reactive-ion etching (RIE) [10]. Conventional bottom-up bioprocess, such as cell cultivation, provides an alternative approach of fabricating nanoscale structure with low cost and less complexity.

Nature may provide abundant and inexpensive sources for photonic-crystal-like structures. Diatoms are photosynthetic marine micro-organisms that create their own skeletal shells of hydrated amorphous silica, called frustules, which possess hierarchical nano-scale photonic crystal features [11]-[12]. Such nano-biosilica is formed by a bottom-up approach at ambient temperature and pressure when a diatom takes up water soluble silicic acid from the environment, which is precipitated into amorphous silica within an intracellular nano-bioreactor. Diatom frustules are low-cost, nanoscale and hierarchically structured materials that could potentially revolutionize the fabrication of photonic crystals. Potential applications of diatoms for the detection of antibodies, solar cells, electroluminescent display, high surface area battery materials, photoluminescence, and nanoplasmonic photonic devices have been explored by many researchers [13]-[19]. Our previous work theoretically and experimentally demonstrated that the photonic-crystal-like structure of a diatom frustule can provide GMRs in the visible wavelength range [20]. NPs-on-diatom nanostructures provide enhanced plasmonic resonances at visible wavelengths due to the intrinsic surface plasmonic resonances of silver (Ag) NPs coupled with the GMRs of diatom frustules [20]. Such NPs-on-diatom nanostructures with enhanced LSPs are expected to have a tremendous engineering potential for SERS sensors.

In this paper, we systematically investigate the application of the NPs-on-diatom nanostructure for SERS sensing. By coating Ag NPs onto diatom frustules using a self-assembly method, we observe enhanced SERS signals due to the coupling of the LSPs with the GMRs of the photonic structure of the diatom frustules. Stronger optical scattering was directly observed from the NPs on a diatom than that on the glass substrate via a high magnification microscope. SERS detection of Rhodmine 6G (R6G) molecules at resonance wavelength (532 nm) shows that the NPs-on-diatom structure provides 4-6× improvement in sensitivity when compared to the NPs-on-glass structure that is confirmed by confocal SERS

The contact author Dr. A. X. Wang is with the Department of Electrical Engineering and Computer Science, Oregon State University, OR 97331 USA (e-mail: wang@eecs.oregonstate.edu)

Dr. Gregory L. Rorrer is with School of Chemical, Biological & Environmental Engineering Oregon State University, Oregon State University, OR 97331 USA (e-mail: rorrergl@engr.orst.edu)

mapping. When excited by nonresonance wavelength (785nm), the NPs-on-diatom structure provides 9-12× improvement in SERS sensitivity.

## II. Sample Preparation

### A. Diatom Fabrication

*Pinnularia* sp. is a single-celled marine diatom with an elliptical cell shape. A representative scanning electron microscopy (SEM) image of the diatoms is presented in Fig. 1(a). The cell dimensions for this species are ~30 µm along the major axis and ~5 µm along the minor axis. Biogenic silica materials were grown on glass substrates and the organic cell materials were removed. The details of the cell cultivation of diatom frustules can be found in our previous work [20]. The structure of a diatom frustule with submicron features is shown in the SEM image in Fig. 1(b). The diatom frustule consists of two-dimensional arrays of sub-micron pores with diameters of ~200 nm. The primary pores of the frustule were lined with a thin layer of biosilica containing several subpores with diameters of 25-50 nm. The nominal lattice constant of the nanophotonic structure is 340 ± 30 nm with refractive index ranging between 1.43-1.48 [12].

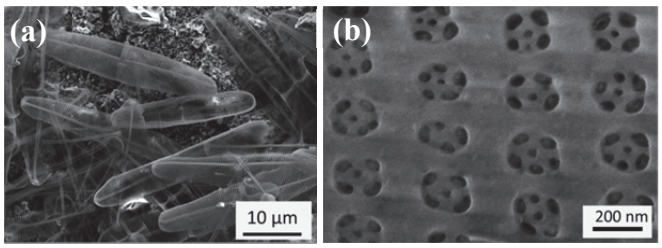


Fig. 1. Representative SEM images of *Pinnularia* sp. showing (a) an overview of diatom frustules; (b) nanoscale arrays of primary pores on a frustule with 50-80 nm subpores.

### B. Silver Self-Assembly to Amine-Functionalized Diatom Biosilica

The Ag NPs solution was prepared by the Lee-Mesel Method [20]. 250 mL of 1 mM silver nitrate aqueous solution was heated to boiling in an oil bath. Sodium citrate (1%, by weight) solution of 5 mL was added to the silver nitrate solution as soon as the boiling occurred, and heating condition was continued for an additional 1 hour. The color of the solution turned into grayish yellow which indicated that the reaction was completed.

The Ag NPs were self-assembled onto a diatom-coated glass substrate modified with aminopropyltriethoxylsilane (APTES) [21]. First, the substrate was immersed in a RCA solution (1:1:5 $H_2O_2/NH_4OH/H_2O$) for 1 hour at 70 ˚C. The sample was then rinsed with deionized water and methanol. This pretreatment created abundant hydroxyl groups on the diatom frustule and the substrate surface. After cleaning, the diatom samples were immersed in APTES (10%, by weight in methanol) solution for 5 hours, followed by rinsing with copious methanol and deionized water. . The APTES was attached to the sample surface by the hydroxyl groups created from the previous treatment. The sample was immersed into an Ag colloidal suspension overnight (12 hours) and rinsed with deionized water and dried with high-purity nitrogen

Ag colloids prepared by the Lee-Mesel method yield Ag NPs with a wide range of sizes (50-150 nm), geometries and aggregation states. NPs of various aggregation states including isolated NPs, NP dimers, trimers, short chains and nanorods are distributed on top of the frustule and substrate respectively, as shown in Fig. 2(a) and Fig. 2(b) . It has been studied that the nanoparticle size and shape are less crucial than the size of interparticle gaps in the SERS measurement [23]. Previous studies suggest that the enhancement factors for the NPs significantly depend on the formation of optical hot-spots, where two particles are in a few nanometers proximity [23]-[24], which were randomly formed on diatom frustules and the glass substrate, as shown in the SEM images. Fig. 2(c) and Fig. 2(d) show the high-magnification optical microscopy images focused on a diatom frustule and on the glass substrate, respectively. These images directly compare the optical scattering from the Ag NPs on the diatom frustule and the Ag NPs on the flat glass substrate, which suggest that the LSPs are significantly enhanced by the diatom frustule.

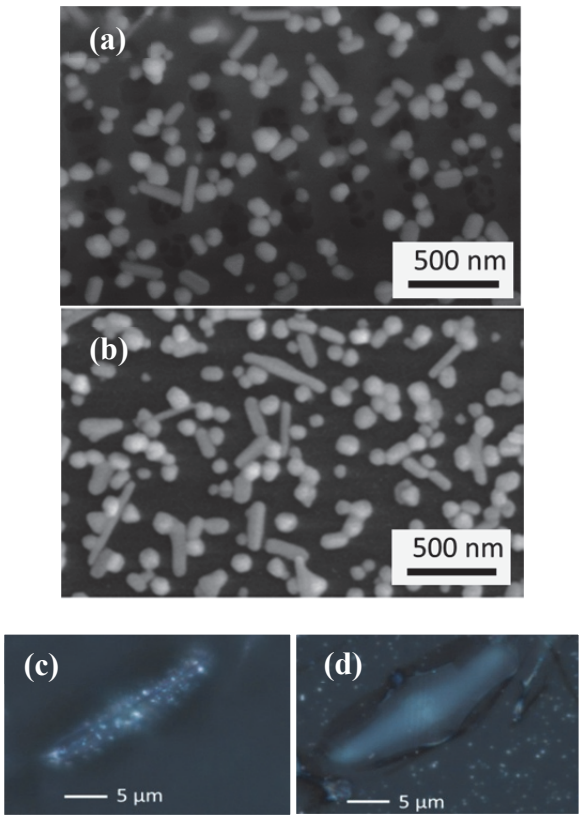


Fig. 2 (a) SEM image of Ag NPs on the diatom frustule. (b) SEM image of Ag NPs on the glass substrate. (c) optical image of Ag NPs on a diatom frustule with focal plane at the diatom surface; (d) optical image of Ag NPs with focal plane on the glass substrate.

## III. Results and Discussion

### A. SERS Measurement under resonance condition

In order to evaluate the sensitivity of the SERS sensor based on nanobiosilica with self-assembled Ag NPs, spectra of R6G molecules were collected using the excitation light at molecular resonance wavelength (532 nm) and nonresonance wavelength (785 nm) on the NPs-on-diatom and NPs-on-glass samples, respectively. R6G is a strong fluoresce dye

which shows a molecular resonance Raman scattering effect with the excitation wavelength at 532 nm. In our SERS measurement, R6G molecules in ethanol were drop-coated on the glass substrate with diatom frustules and then evaporated to dryness. Molecular resonance SERS microscopy was performed using a Horiba Jobin-Yvon HR800 confocal Raman spectrometer equipped with a 532 nm diode laser through a notch filter. During the measurement, the confocal pin-hole size was set at 100 µm. A 50× objective lens (NA = 0.75) was used to focus the excitation light to a 2 µm spot totally within a single diatom frustule for each spectrum acquisition. Raman signals were detected by a Synapse charge-coupled device (CCD) detector. Fig. 3(a) shows the single-point SERS signals measured on the flat glass substrate and on the diatom frustule respectively. SERS signals of the NPs-on-diatom structure show 3.6-6.2× enhancement compared with that on the NPs-on-glass substrate for major R6G Raman peaks at 614 $cm^{-1}$, 1368 $cm^{-1}$, 1511 $cm^{-1}$, 1578 $cm^{-1}$ and 1651 $cm^{-1}$. The additional enhancement of Raman signals is attributed to the enhanced LSPs due to the presence of the diatom frustule. R6G Raman spectra have been studied in the concentration range of $10^{-9}$ to $10^{-4}$ M. The Raman band at 1368 $cm^{-1}$ was used to probe the strength of the SERS of which the intensity were plotted in Fig. 3(b). The Raman signals increase from $10^{-8}$ M to $10^{-5}$ M after which the Raman intensity decreases at $10^{-4}$ M. 4.1-6.4× enhancement factors of the Raman signals between the NPs-on-diatom and the NPs-on-glass samples were observed throughout the concentration range of $10^{-8}$ M to $10^{-5}$ M, which are attributed to the GMRs of the diatom frustule. When further increasing the concentration from $10^{-5}$ M to $10^{-4}$ M, more R6G molecules were attached to the nano-corrugated surface of the frustule, which resulted in a significant increase of florescence baseline. In this case, the florescence signals competed with the SERS signals and degraded the SERS intensity. Therefore, the decreasing of Raman signal intensity was observed after subtracting the florescence baselines when we increased the R6G molecules to a higher concentration above $10^{-4}$ M.

The intensity of SERS signals depend on the local R6G concentration, the aggregation states of the Ag NPs, and the surfaces of diatom frustules. By mapping a large area of the substrate which includes a diatom frustule as well as some flat glass surface, we are able to investigate the average effects of these factors on SERS signal intensity. A total of 625 SERS spectra were acquired within the scanning range of 50 µm×50 µm that is divided into an acquisition area of 25 × 25 grids, as shown in Fig. 3(c) and Fig. 3(d). The SERS mapping results of the intensity of 1368 $cm^{-1}$ Raman peak exhibit a pattern of increased signal intensity which correlates with the shape of the diatom frustule that is observed in the corresponding optical image. The average measured SERS signal intensity for the NPs-on-diatom area was 2094 ± 1531, whereas the average signal intensity of the NPs-on-glass area was 488 ± 472. The presence of the diatom photonic structures results in an average SERS enhancement factor of 4.3× compared to that on the flat glass substrate. This SERS mapping measurement suggests that highly enhanced surface plasmons are localized on the diatom frustules, achieving a diatom-based SERS sensor that can substantially enhance the SERS sensitivity. The enhancement factor was strongly correlated to the enhanced electric field around the Ag NPs due to the GMRs of the photonic crystal structure.

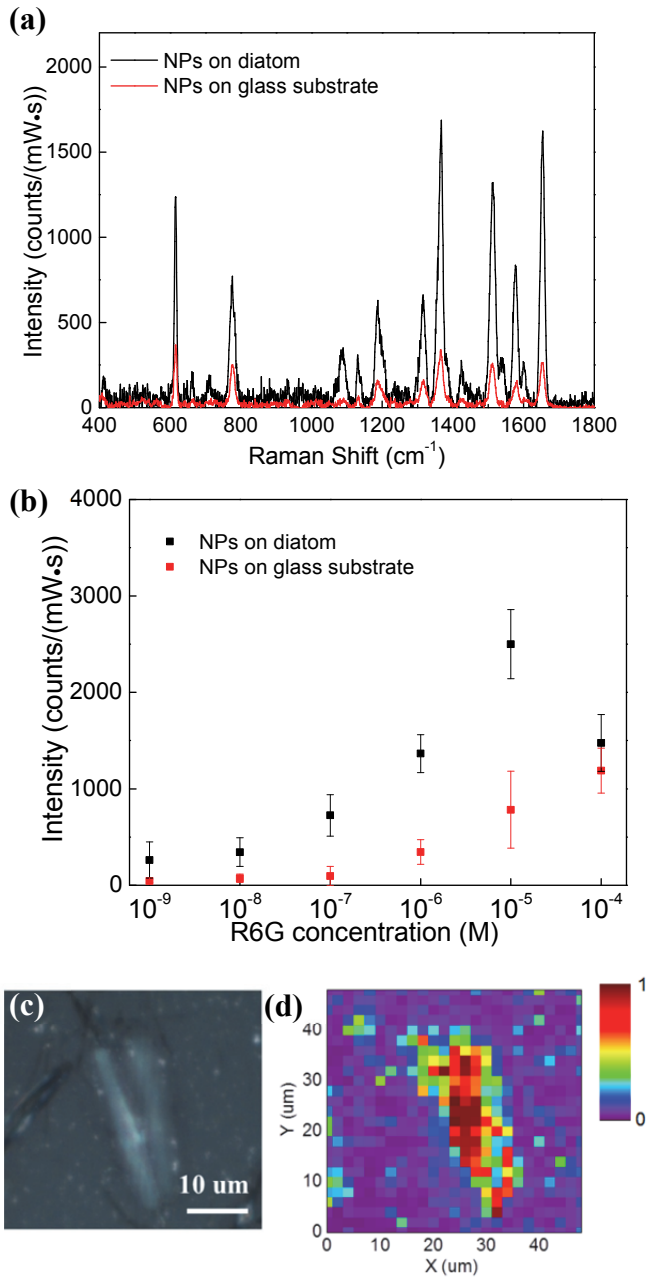


Fig. 3 (a) SERS spectra of 1µM R6G coated on Ag NPs-on-diatom (black) and Ag NPs-on-glass (red); (b) Intensities of Raman band at 1368 $cm^{-1}$ for different R6G concentrations. (c) Optical image of the sensing area scanned for SERS enhancement; and (d) Mapping of Raman signal intensity at 1368 $cm^{-1}$. During the measurement, the excitation power was set at 1.2 mW and integration time was 1 second.

In order to verify whether the additional enhancement of Raman signals comes from the photonic crystal structure of the diatom frustules, we mapped the Raman signals with respect to the NPs density. Such analysis will rule out the effect of NP

density variation on diatom and glass substrate[25]-[26]. SERS mapping signals were collected in a deterministic acquisition area as shown in a SEM image in Fig. 4 (a), from which the NP density can be accurately obtained. To prepare the sample, the NP solution was diluted by 1:10 with water. Due to the relatively large sizes of the Ag NPs, the NPs were excluded from the nanopores and were majorly assembled on the surface of the diatom frustules. The SEM image shows that in the SERS mapping area, Ag NPs were uniformly distributed onto the diatom and glass substrate with an average density of 7/μm$^2$. This conclusion is also confirmed by the zoomed SEM images as shown in Fig. 2 (a) and (b), which show that there is no statistic difference of the NP density and morphologies between the glass and diatom substrate. A SERS map of 6 ×6 grids (36 mapping points, grid size: 2μm) for R6G was acquired. The Raman peak at 1368 cm$^{-1}$ was analyzed to generate the map and the mapping intensities were normalized by the NP densities in each grid, which are shown in Fig. 4(b). The diatom photonic crystal structure results in an average SERS enhancement factor of 3.8× when compared to that on the flat glass substrate. In some area, the enhancement factor can be as high as 7.2×. Therefore, it is unequivocal to conclude that the GMR effect of diatom frustules can enhance the SERS signals.

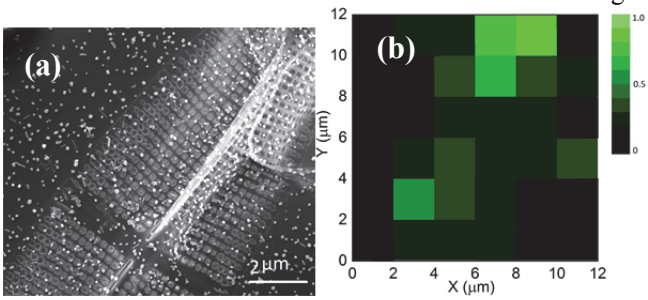


Fig. 4 (a) SEM image of the acquisition area for SERS mapping (b) The map of Raman signal intensity at 1368 cm-1 normalized by the NP numbers in each grid showing in the SEM image. The excitation power was set at 1.2 mW and the integration time was 1 second.

### *B. SERS Measurement under nonresonance condition*

SERS spectra were recorded using 785 nm excitation wavelength to avoid a complex interference of molecular resonance Raman scattering effect since the excitation energy of 785 nm is away from the electronic absorption band of R6G, which results in nonresonance Raman scattering. Due to the fact that the glass substrate displays strong florescence background under the 785 nm wavelength excitation, diatom frustules in aqueous solution were drop-coated on non-florescent quartz substrate for the measurement. The diatom frustules were annealed at 425 ˚C in air for 1 hour in order to improve the adhesion to the quartz substrate. The fabrication process of self-assembled NPs onto a diatom-coated quartz substrate is identical to the diatom-coated glass substrate as described in Section II. Fig. 5(a) shows the nonresonance SERS spectra under the 785 nm excitation light from a diode laser. The SERS spectra indicates that the Raman signal intensity is enhanced by 8.7-13.3× on the diatom frustule compared with the flat quartz substrate for the Raman bands of 776 cm$^{-1}$, 1183 cm$^{-1}$, 1315 cm$^{-1}$, 1368 cm$^{-1}$, and 1511 cm$^{-1}$. The larger additional enhancement factors from diatom frustules to the R6G Raman signals under nonresonance condition compared with resonance condition can be explained by the difference between resonance and nonresonance Raman scattering by surface plasmons [27]. Resonance Raman process is subjected to quenching effect, where an additional loss is introduced for the energy stored in coherent oscillations of molecular dipoles at the excitation wavelengths in the presence of LSP enhancement and GMR enhancement [27]. Compared with resonance Raman process which limits the attainable enhancement, such quenching effect is absent in normal nonresonance Raman scattering.

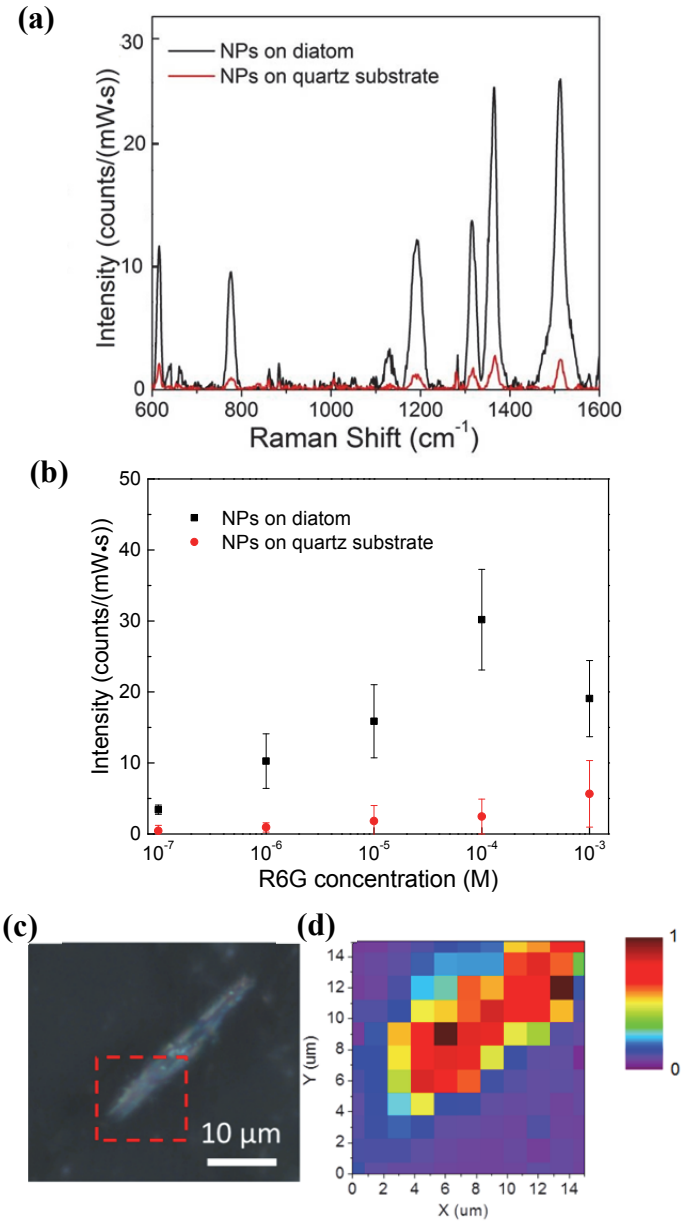


Fig. 5(a) SERS spectra of 100 μM R6G coated on Ag NPs-on-diatom (black) and Ag NPs-on-quartz (red); (b) Intensities of Raman band 1368 cm$^{-1}$ for different R6G concentrations. (c) Optical image of the area scanned for SERS measurement; and (d) Map of Raman signal intensity at 1368 cm$^{-1}$. During the measurement, the integration time was 60 second and the grating groove density was set at 300/mm. The excitation power was 2.1 mW.

The intensities of the Raman band at 1368 cm$^{-1}$ were plotted in

the concentration ranges from $10^{-7}$ M to $10^{-3}$ M in Fig 5(b). The average enhancement effect to the Raman signals was observed throughout the concentration range of $10^{-7}$ M to $10^{-4}$ M with enhancement factors of 8.9-12.3× between NPs-on-diatom and NPs-on-quartz. For the SERS mapping measurement, an area of 15 μm×15 μm in Fig. 5(c) was scanned to generate a map in Fig. 5(d). The average measured SERS signal intensity for the NPs-on-diatom area was 4187 ± 2753, which shows an average signal enhancement of 9.2× compared to quartz substrate whereas the average signal intensity of the NPs-on-quartz area was 457 ± 312. Such enhancement factor for nonresonance SERS is more desirable for biosensing application as fluorescence interference can be avoided compared with resonance SERS.

### *C. Evaluation of Guided Mode Resonance from Diatom Frustules*

Our previous research presented the GMRs from diatom frustules by measuring the extinction spectrum at visible wavelengths [19], which shows a broad, low-Q resonance that can be coupled with the plasmonic resonances of Ag NPs. In order to confirm the effective enhancement at both 532 nm and 785 nm, a broadband white light source with Vis-NIR (visible to near infrared) output was used as the excitation source. Details of the experimental setup can be found in Ref [19]. From the extinction spectra as shown in Fig. 6(a), the diatom frustule increases the optical extinction ratio of the NPs by 2× compared to Ag NPs on the glass substrate from 500 nm to 850 nm wavelength.

The Raman scattering signals of R6G molecules on the diatom and the glass substrate were also investigated respectively without plasmonic enhancement from NPs in order to confirm the contribution of GMRs from diatom frustules. Raman signals of 5mM R6G from the diatom frustule (black) and glass substrate (red) are plotted in Fig. 6(b). The amplitude of the Raman signals is very weak, but it still clearly shows that there is 3.9 × enhancement for the Raman peak at 1368 $cm^{-1}$ from the diatom frustule compared to that from the glass substrate. We attribute this enhancement to the GMRs of the diatom frustules.

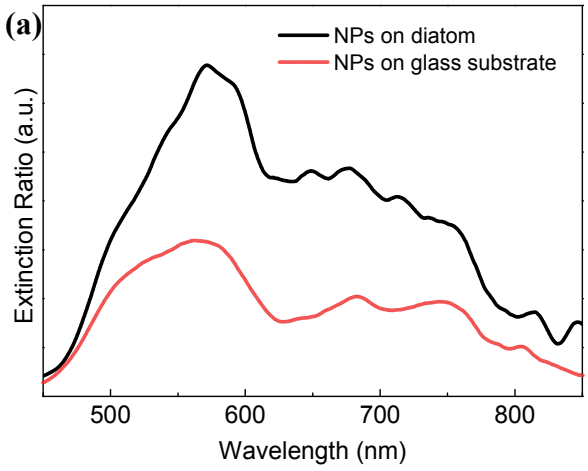


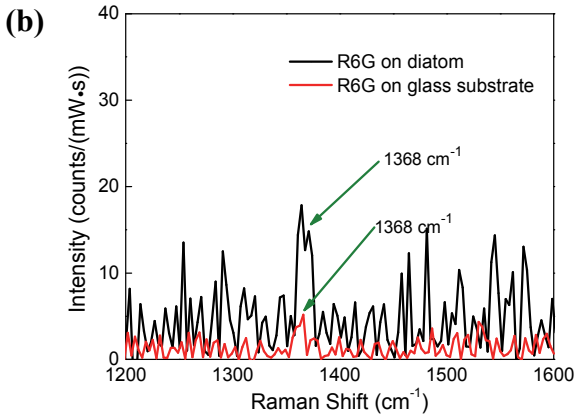


Fig. 6. (a) Measured extinction spectra of NPs on a diatom frustule (black) and Ag NPs on glass substrate (red). (b) Raman spectra of 5 mM R6G on diatom (black) and glass substrate (red). During the Raman measurement, the excitation power was set at 1.2 mW and integration time was 5 second.

## IV. Conclusion

In conclusion, we have demonstrated that the guided-mode resonances of diatom frustules can effectively couple with the localized surface plasmons of the Ag NPs, which will increase the average enhancement factor of SERS sensors. An additional enhancement factor of the SERS signals of 4-6× was observed for resonance condition when the molecular concentrations are from $10^{-9}$ M to $10^{-5}$ M. Under nonresonance condition, the Raman enhancement factor of 9-12× was obtained over the concentrations from $10^{-7}$ M to $10^{-4}$ M. Such NPs-on-diatom SERS substrate will have significant potentials in chemical and biochemical diagnostics, pathogen detection, and environmental protection.

## Acknowledgment

*A. X. Wang would like to acknowledge Marine Polymer Technologies, Inc. and partial support of the National Institute of Health under grant No. of 9R42ES024023-02 to F Ren. G.L. Rorrer acknowledges support of this research by the National Science Foundation (NSF) through the Emerging Frontiers in Research and Innovation (EFRI) program, award number 1240488. The authors would like to thank Xiangyu Wang for the help of taking SEM images of the samples.*

## References

[1] J. Homola, S. S. Yeea, and G. Gauglitzb, "Surface Plasmon Resonance Sensors: Review," *Sens. Actuators, B*, vol. 54, pp. 3-15, Jan. 1999.
[2] . T., Vo-Dinh, "Surface-enhanced Raman spectroscopy using metallic nanostructures," *TrAC, Trends Anal. Chem.*, vol. 17, no. 8 pp. 557-582, Sep.1998.
[3] K. Kneipp, Y. Wang, H. Kneipp, L. T. Perelman, I. Itzkan, R. Dasari, and M. S. Feld, "Single molecule detection using surface-enhanced Raman scattering (SERS)," *Phys. Rev. Lett.*, vol. 78, pp. 1667-1670, Mar. 1997.
[4] S. Nie and S. R. Emory, "Probing Single Molecules and Single Nanoparticles by Surface-Enhanced Raman Scattering" *Science* vol. 275, no. 5303, pp. 1102-1106, Feb. 1997.
[5] M. Barth, S. Schietinger, S. Fischer, J. Becker, N. Nusse, T. Aichele, B. Lochel, C. Sonnichsen, and O. Benson. "Nanoassembled plasmonic-photonic hybrid cavity for tailored light-matter coupling." *Nano Lett.*, vol. 10, no. 3, pp. 891-895, Feb. 2010.
[6] M. A. Schmidt, D. Y. Lei, L. Wondraczek, V. Nazabal, and S. A. Maier. "Hybrid nanoparticle-microcavity-based plasmonic nanosensors with

improved detection resolution and extended remote-sensing ability." *Nat. Commun.*, vol. 3, pp. 1108-1-1108-7, Oct. 2012.

[7] X. Xu, D. Hasan, L. Wang, S. Chakravarty, R. T. Chen, D. L. Fan, and A. X. Wang. "Guided-mode-resonance-coupled plasmonic-active $SiO_2$ nanotubes for surface enhanced Raman spectroscopy, *Appl. Phys. Lett.* vol. 100, pp. 191114-1-191114-5, May 2012.

[8] I. M. White, J. Gohring, and X. Fan. "SERS-based detection in an optofluidic ring resonator platform." *Opt. Exp.*, vol. 15, no. 25, pp. 17433-17442, Dec. 2007.

[9] M. Hu, D. Fattal, J. Li, X. Li, Z. Li, and R. S. Williams, "Optical properties of sub-wavelength dielectric gratings and their application for surface-enhanced Raman scattering," *Appl. Phys. A*, vol. 105, no. 2, pp. 261-266, Sep. 2011.

[10] C. Cheng, and A. Scherer, "Fabrication of photonic band gap crystals," *J. Vac. Sci. Technol.*, vol. 13, no.6, pp. 2696-2700, Nov. 1995.

[11] F. E Round, R. M Crawford, D. G Mann, The Diatoms, Biology & Morphology of the Genera, Cambridge University Press, 1990.

[12] C. Jeffryes, R. Solanki, Y. Rangineni,; W. Wang, C. H. Chang, and G. L. Rorrer, "Electro-luminescence and photoluminescence from nanostructured diatom frustules containing metabolically inserted Germanium," *Adv. Mater.*, vol. 20, pp. 2633-2637, Jun. 2008.

[13] R. Gordon, D. Losic, M. A. Tiffany, S. S. Nagy, and F. A. Sterrenburg, "The glass menagerie: diatoms for novel applications in nanotechnology," *Trends Biotechnol.*, vol. 27, pp.116-127, Feb. 2009.

[14] C. Jeffeyes, J. Campbell, H. Li, J. Jiao, and G.L. Rorrer, "The potential of diatom nanobiotechnology for applications in solar cells, batteries, and electroluminescent devices," *Energy Environ. Sci. 4*, pp.v3930-3941, Sep. 2011.

[15] D. K. Gale, T. Gutu, J. Jiao, C.H. Chang, and G. L. Rorrer, "Photoluminescence detection of biomolecules by antibody-functionalized diatom biosilica," *Adv. Funct. Mater.*, vol. 19, pp. 926-933, Mar. 2009.

[16] T. Qin, T. Gutu, J. Jiao, C. H. Chang, and G. L. Rorrer, "Photoluminescence of Silica Nanostructures from Bioreactor Culture of Marine Diatom Nitzschia frustulum," *J. Nanosci. Nanotechnol.*, vol. 8, pp. 2392-2398, Feb. 2008.

[17] Y. Yu, J. Addai-Mensah and D. Losic, "Synthesis of self-supporting gold microstructures with three-dimensional morphologies by direct replication of diatom templates," *Langmuir*, vol. 26, pp. 14068-14072, Jul. 2010.

[18] D. Losic, J. G. Mitchell, R. Lal, and N. H. Voelcker, "Rapid fabrication of micro- and nanoscale patterns by replica molding from diatom biosilica," *Adv. Funct. Mater.*, vol. 17, pp. 2439-2446, Sep. 2007.

[19] T. Fuhrmann, S. Landwehr, M. El Rharbi-Kucki, and M. Sumper, "Diatoms as living photonic crystals," *Appl. Phys. B-Lasers O.*, vol. 78, pp. 257-260, Jan. 2004.

[20] F. Ren, J. Campbell, X. Wang, G. L. Rorrer, , and A. X. Wang, "Enhancing surface plasmon resonances of metallic nanoparticles by diatom biosilica," *Opt. Exp.*, vol. 21, no. 13, pp. 15308-15313, Jun. 2013.

[21] P. C. Lee, and D. J. Meisel. "Adsorption and surface-enhanced Raman of dyes on silver and gold sols," *Phys. Chem.*, vol. 86, pp. 3391-3395, Aug. 1982.

[22] S. Liu, T. Zhu, R. Hua and Z. Liu, "Evaporation-induced self-assembly of gold nanoparticles into a highly organized two-dimensional array," *Phys. Chem. Chem. Phys.*, vol. 4, pp. 6059-6062, Nov. 2002.

[23] K. L.Wustholz, A.-I. Henry, J. M. McMahon, R. G. Freeman, N. Valley, M. E. Piotti, M. J. Natan, G. C. Schatz, and R. P. Van Duyne. "Structure-activity relationships in gold nanoparticle dimers and trimers for surface-enhanced Raman spectroscopy." *J. Am. Chem. Soc.*,vol. 132, no. 31, pp.10903-10910, Jul. 2010.

[24] M. I. Stockman, L. N. Pandey, and T. F. George, "Inhomogeneous localization of polar eigenmodes in fractals," *Phys. Rev. B Condens. Matter* vol. 53, no.5, pp. 2183-2186, Feb. 1996.

[25] Jack J. Mock, Ryan T. Hill, Aloyse Degiron, Stefan Zauscher, Ashutosh Chilkoti, and David R. Smith. "Distance-dependent plasmon resonant coupling between a gold nanoparticle and gold film." *Nano lett.* vol. 8, no.8, 2245-2252, Jul. 2008.

[26] J. D. Caldwell, O. Glembocki, F. J. Bezares, N. D. Bassim, R. W. Rendell, M. Feygelson, M. Ukaegbu, R. Kasica, L. Shirey, and C. Hosten. "Plasmonic nanopillar arrays for large-area, high-enhancement surface-enhanced Raman scattering sensors." *ACS nano* vol.5 no.5, pp.4046-4055, Apr. 2011.

[27] G. Sun, and J. B. Khurgin. "Origin of giant difference between fluorescence, resonance, and nonresonance Raman scattering enhancement by surface plasmons." *Phys. Rev. A*, vol. 85, no. 6, pp. 063410-1-063410-8, Jun. 2012.

**Fanghui Ren** (S'2012) received her B.S. degree in Physics from Southwest University, Chongqing, China in 2010, and the M.S. degree in electrical and computer engineering from Oregon State University, Corvallis, in 2012. She is currently pursuing a Ph.D. degree in electrical and computer engineering at Oregon State University, Corvallis, OR.
Her research interests include hybrid biological-plasmonic optical sensors, photonic crystal and surface plasmonic devices for optical communication.

**Jeremy Campbell** received his B.S. degree in Chemical Engineering from Oregon State University, Corvallis, in 2006, and his M.S. degree in Chemistry from the University of Oregon, Eugene in 2009. He is currently pursuing a Ph.D. degree in Chemical Engineering at Oregon State University, Corvallis, OR.
His research interests include the optical properties of diatom biosilica for solar energy conversion and strategies for biological thin film formation for engineering applications.

**Gregory L. Rorrer** has a B.S. degree in Chemical Engineering from the University of Michigan, and a PhD degree in Chemical Engineering from Michigan State University.
He is currently Professor and Head of the School of Chemical, Biological, and Environmental Engineering at Oregon State University, and holds the James & Shirley Kuse Chair in Chemical Engineering. From 2009 to 2011, he served as the program director of the Energy for Sustainability program within the Engineering Directorate at the National Science Foundation (NSF). His expertise encompasses bioprocess engineering, renewable energy and fuels, microchannel reactors, and biological fabrication of nanomaterials. His current research focuses on harnessing the unique biosynthetic capacities of photosynthetic algae for applications in nanotechnology, bioenergy, bioactive compound production, and environmental remediation. The Rorrer Lab is currently supported by grants from the NSF Emerging Frontiers in Research & Innovation (EFRI) program, the U.S. Office of Naval Research (ONR), and private industry. He is also a co-author on the 4th and 5th editions of the widely-used textbook Fundamentals of Momentum, Heat, and Mass Transfer.

**Alan X. Wang** received his B.S. degree from Tsinghua University, and M.S. degree from the Institute of Semiconductors, Chinese Academy of Sciences, Beijing, P.R. China, in 2000 and 2003, respectively, and his Ph.D. degree in Electrical and Computer Engineering from the University of Texas at Austin in 2006.
He is an Assistant Professor in the School of Electrical Engineering and Computer Science, Oregon State University since 2011. From 2007 to 2011, he was a research scientist at Omega Optics, Inc. He has authored or coauthored more than 40 journal papers, and more than 50 conference papers. He holds 3 U.S. patents. His research interest covers board level optical interconnects, micro- and nano- photonic devices, RF photonics, and optical sensing technologies including IR spectroscopy and Raman scattering for biomedical research and environmental protection. He is a member of the Institute of Electrical and Electronics Engineers (IEEE), the Optical Society of America (OSA), and the International Society for Optical Engineering (SPIE). He served as program committee members and session chairs for SPIE Photonic West conference in Optoelectronic Interconnects and Component Integration XI in 2009~2011, and conference chair for Photonics Asia in 2010.